The American Journal of Pathology, Vol. 174, No. 1, January 2009

DOI: 10.2353/ajpath.2009.080385

Vascular Biology, Atherosclerosis and Endothelium Biology

Valproate Attenuates Accelerated Atherosclerosis in Hyperglycemic ApoE-Deficient Mice

Evidence in Support of a Role for Endoplasmic Reticulum Stress and Glycogen Synthase Kinase-3 in Lesion Development and Hepatic Steatosis

Anna J. Bowes,* Mohammad I. Khan,† Yuanyuan Shi,† Lindsie Robertson,* and Geoff H. Werstuck*†‡

From the Department of Biochemistry and Biomedical Sciences, the Henderson Research Centre,† and the Department of Medicine,‡ McMaster University, Hamilton, Ontario, Canada*

We have previously shown that glucosamine promotes endoplasmic reticulum (ER) stress in vascular cells leading to both inflammation and lipid accumulation—the hallmark features of atherosclerosis. Pretreatment with glycogen synthase kinase (GSK)-3 inhibitors protects cultured cells from ER stress-induced dysfunction. Here we evaluate the potential role of GSK-3 on the pro-atherogenic effects of hyperglycemia and ER stress. We show that GSK-3-deficient mouse embryonic fibroblasts do not accumulate unesterified cholesterol under conditions of ER stress. Furthermore, GSK-3 inhibitors, including valproate, attenuate ER stress-induced unesterified cholesterol accumulation in wild-type mouse embryonic fibroblasts. *In vivo* we show that hyperglycemic apoE-deficient mice have accelerated atherogenesis at the aortic root compared with normoglycemic control mice. Mice fed a diet supplemented with 625 mg/kg valproate have significantly reduced lesion volume relative to nonsupplemented controls. Valproate supplementation has no apparent effect on the plasma levels of either glucose or lipids or on the expression of diagnostic markers of ER stress in the lesion. Significant reductions were observed in total hepatic lipids (>50.4%) and hepatic GSK-3β activity (>55.8%) in mice fed the valproate diet. In conclusion, dietary supplementation with low levels of valproate significantly attenuates atherogenesis in hyperglycemic apoE-deficient mice. The *in vivo* anti-atherogenic effects of valproate are consistent with its ability to inhibit GSK-3 and interfere with pro-atherogenic ER stress signaling pathways *in vitro*. *(Am J Pathol 2009, 174:330–342; DOI: 10.2353/ajpath.2009.080385)*

Individuals with diabetes have a twofold to fourfold increased risk of coronary heart disease and a fourfold increased risk of mortality from heart disease.[1] Chronically elevated blood glucose is a common characteristic of all forms of diabetes, and there is a strong correlation between hyperglycemia and macrovascular disease.[2–4] However, despite a tremendous amount of research, the molecular mechanisms that link diabetes to the development of cardiovascular disease are not completely understood.

It has become increasingly evident that disruption of endoplasmic reticulum (ER) homeostasis and/or the activation of the unfolded protein response (UPR) can play a significant role in the development and progression of atherosclerotic lesions.[5] Independent cardiovascular risk factors including hyperhomocysteinemia, obesity, cholesterol, and diabetes mellitus have been linked to elevated levels of diagnostic markers of ER stress and the induction of the UPR.[6–9] The mechanisms by which conditions of ER stress promote these downstream, pro-

Supported by the Heart and Stroke Foundation of Ontario (grant NA5556/T6104), the Canadian Institutes of Health Research (grant MOP-62910), the Heart and Stroke Foundation of Canada (New Investigators grant to G.H.W.), the Natural Sciences and Engineering Research Council of Canada (scholarship to A.J.B.), and the Canadian Diabetes Association (scholarship to A.J.B.).

Accepted for publication September 11, 2008.

Supplemental material for this article can be found on *http://ajp.amjpathol.org.*

Address reprint requests to Geoff H. Werstuck, Henderson Research Centre, 711 Concession St., Hamilton, Ontario, Canada, L8V 1C3. E-mail: gwerstuck@thrombosis.hhscr.org.

atherogenic changes are not yet fully understood. We have previously shown that ER stress-inducing agents can promote cellular responses that represent the hallmark features of atherosclerosis, including apoptosis, cholesterol accumulation, and activation of inflammatory pathways in cultured human aortic smooth muscle cells (HASMCs) and HepG2 cells.[9,10] We have also shown that glucosamine, a downstream metabolite of glucose, is an ER stress-inducing agent and that the accumulation of glucosamine in vascular tissue is associated with ER stress and accelerated atherosclerosis in hyperglycemic mice.[9]

Glycogen synthase kinase (GSK)-3α and -3β are serine/threonine kinases that are regulated by mitogens and growth factors including insulin, insulin-like growth factor-1, and epidermal growth factor, as well as conditions of cellular stress including heat shock and oxidative stress. A partial list of substrates includes the translation initiation factor eIF2$\beta\varepsilon$, transcription factors CREB, c-Jun, c-Myc, c-Myb, HSF-1, NFAT1, β-catenin, cyclin D1, ATP-citrate lysase, and the amyloid precursor protein tau.[11,12] GSK-3 plays a central role in many cellular processes including glycogen metabolism, gene expression, cell cycle regulation, and cell proliferation. GSK-3 appears to play a fundamental role in the promotion of apoptotic signaling,[13,14] and the GSK-3β isoform is essential for the hepatoprotective activation of nuclear factor-κB.[15,16] Disruption and/or dysregulation of GSK-3 activity has been implicated in several pathophysiological processes and diseases including diabetes mellitus, cardiac hypertrophy, Alzheimer's disease, bipolar disorder, and cancer.[17–21]

Recent findings suggest that GSK-3 may be involved in the cellular response to conditions of ER stress. First, GSK-3 is involved in cellular processes that are induced by ER stress including apoptosis and inflammation.[15,22] Second, ER stress-inducing agents have been shown to increase GSK-3 activity in rat cerebral cortical cells, mouse insulinoma cells, and mouse embryonic fibroblasts (MEFs).[22–26] Third, increased GSK-3 activity has been observed in human muscle and mouse β-cells under hyperglycemic conditions.[20,27–29] Finally, we have shown that small molecule inhibitors of GSK-3 attenuate ER stress-induced apoptosis and lipid accumulation *in vitro*.[10]

We hypothesize that hyperglycemia accelerates atherogenesis by a pathway that involves ER stress-induced activation of GSK-3 and that inhibition of GSK-3 will slow the progression of lesion development. Here we investigate the role of GSK-3α and -3β in ER stress-induced unesterified cholesterol accumulation *in vitro* and examine the effect of one inhibitor of GSK-3, valproate, on the development of hepatic steatosis and accelerated atherosclerosis in a diabetic apolipoprotein E-deficient (apoE$^{-/-}$) mouse model.

Materials and Methods

Cell Culture and Treatment Conditions

Wild-type, GSK-3$\alpha^{-/-}$, and GSK-3$\beta^{-/-}$ MEFs were generous gifts from Dr. Bradley Doble and Dr. James Woodgett (McMaster University, Hamilton, Canada, and University of Toronto, Toronto, Canada). The cells were cultured in Dulbecco's modified Eagle's medium (Life Technologies, Burlington, Canada) containing 10% fetal bovine serum and maintained in a humidified incubator at 37°C with 5% CO_2. Sodium valproate, glucosamine, and filipin were purchased from Sigma (Oakville, Canada). GSK-3 inhibitor II, 3-(3-carboxy-4-chloroanilino)-4-(3-nitrophenyl) maleimide, was purchased from Calbiochem (La Jolla, CA). All compounds were prepared fresh in culture medium, sterilized by filtration, and added to the cell cultures.

Immunoblot Analysis

Antibodies to calreticulin (SPA-600) and the anti-KDEL monoclonal antibody (SPA-827) that recognizes GRP78/BiP were purchased from StressGen Biotechnologies (Victoria, Canada). Anti-GADD153/CHOP (sc-7351) monoclonal antibodies were purchased from Santa Cruz Biotechnology (Santa Cruz, CA). Anti-β-actin (AC-15) antibodies were purchased from Sigma. MEFs were treated with 5 mmol/L glucosamine, 10 μg/ml tunicamycin, or 7 μmol/L A23187 for 18 hours. Total protein lysates (40 μg) from MEFs were solubilized in sodium dodecyl sulfate-polyacrylamide gel electrophoresis sample buffer and separated on sodium dodecyl sulfate-polyacrylamide gels under reducing conditions. After incubation with the appropriate primary and horseradish peroxidase-conjugated secondary antibodies (Life Technologies), the membranes were developed using the Immobilon Western chemiluminescent horseradish peroxidase substrate (Millipore, Billerica, MA).

Unesterified Cholesterol Staining

The accumulation of unesterified cholesterol was determined by filipin staining.[30] MEFs, grown on coverslips, were treated with 4 mmol/L valproate, or 200 nmol/L GSK-3 inhibitor II for 1 hour and challenged with glucosamine (5 mmol/L) for an additional 18 hours. Cells were washed three times with medium 1 (150 mmol/L NaCl, 5 mmol/L KCl, 1 mmol/L $CaCl_2$, 20 mmol/L HEPES pH 7.4, 2 g/L glucose), fixed with 4% paraformaldehyde for 20 minutes at room temperature and then incubated for 2 hours with 50 μg/ml of filipin in medium 1 at room temperature. Cells were washed three times with medium 1 and then filipin-bound unesterified cholesterol complexes were visualized by fluorescence microscopy with excitation at 335 to 385 nm (emission at 420 nm). The accumulation of unesterified cholesterol in primary mouse hepatocytes was quantified using Sigma Plot (Systat Software, Inc., Chicago, IL) as described previously.[10]

Analysis of Unesterified Cholesterol Staining by Fluorescence-Activated Cell Sorting (FACS)

MEFs were grown on 100-mm-diameter culture dishes to 50% confluency and treated with the appropriate drugs as described above. The cells were washed three times with

medium 1, fixed in 4% paraformaldehyde at room temperature for 20 minutes, and incubated with 50 μg/ml filipin for 2 hours at room temperature. Cells were washed with phosphate-buffered saline (PBS), trypsinized, and stored in PBS containing 1% fetal bovine serum. Filipin fluorescence was measured using a FACS VantageSE instrument (Becton Dickinson, San Jose, CA) with 350 to 70 nm UV laser and emission detection at 420 to 460 nm. Data were analyzed using FlowJo software (Treestar, Ashland, OR).

Mouse Models

Five-week-old female apoE$^{-/-}$ (B6.129P2-ApoE^{tm1Unc}) mice were placed on a defined chow diet (TD92078; Harlan Teklad, Madison, WI) and randomly divided into two groups (n = 24 per group). To induce hyperglycemia, one group was injected intraperitoneally with multiple low doses of streptozotocin (STZ) (40 mg/kg) as previously described.[9,31] After 1 week, half of the mice in each group were switched to the control diet supplemented with 625 mg/kg of sodium valproate (TD02165). All mice had unrestricted access to both food and water throughout the study. Mice were sacrificed at 15 weeks of age and blood and tissues were collected for further analysis. To test the effect of lithium, mice with STZ injections were given the control diet supplemented with 4 g of $LiCO_3$/kg chow (TD05217) (Harlan Teklad, Madison, WI). The McMaster University Animal Research Ethics Board approved all procedures.

Plasma Analysis

Random and fasting (12 hours) whole blood glucose levels were measured using a DEX glucometer (Bayer, Pittsburgh, PA). Plasma glucose and lipid levels were determined in nonfasting mice using the colorimetric diagnostic kits for total cholesterol, triglycerides, and glucose purchased from Thermal DMA Inc. (Melbourne, Australia) Plasma valproate concentrations were determined using an AxSYM system (Abbott Laboratories, Mississauga, Canada).

RNA Isolation and Quantitative Reverse Transcriptase-Polymerase Chain Reaction (RT-PCR)

Total RNA was extracted from apoE$^{-/-}$ mouse livers using commercially available TRIzol reagent (Invitrogen, Carlsbad, CA) following the manufacturer's instructions. The concentration and purity of the RNA were determined by measuring the absorbance at 260 and 280 nm. cDNA was synthesized from 2 μg of total RNA using a commercially available kit (High Capacity cDNA reverse transcription kit; Applied Biosystems, Foster City, CA) following the guidelines provided by the manufacturer. Real-time PCR was conducted at the following settings: one cycle at 95°C for 10 minutes, followed by 40 cycles at 95°C for 1 minute, and at 60°C for 1 minute using a GeneAmp 7300 sequence detection system (Applied Biosystems,) and

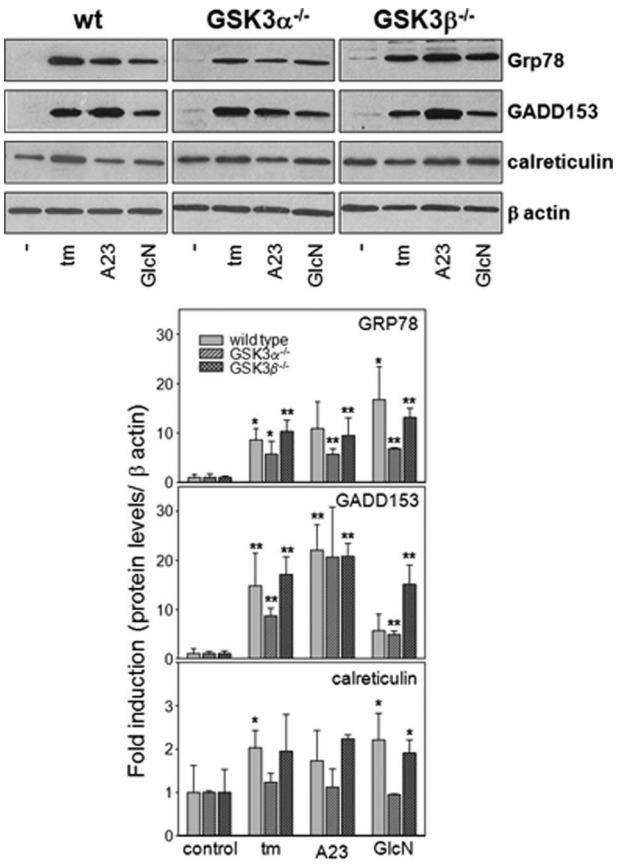

Figure 1. The UPR in GSK-3-deficient MEFs. **A:** Wild-type, GSK-3$\alpha^{-/-}$, and GSK-3$\beta^{-/-}$ MEFs were challenged with ER stress-inducing agents including tunicamycin, A23187, or glucosamine for 18 hours as indicated. Total protein lysates were resolved by sodium dodecyl sulfate-polyacrylamide gel electrophoresis, transferred to nitrocellulose membranes, and immunostained with antibodies against GRP78/BiP, GADD153, calreticulin, or β-actin. **B:** The amount of each protein normalized to β-actin and averaged over three independent experiments was quantified by densitometry. $^*P < 0.05$, $^{**}P < 0.01$ relative to untreated controls.

SYBR GreenER qPCR SuperMix for ABI Prism (Invitrogen). Template cDNAs were amplified using the following primers: for sterol regulatory element binding protein (SREBP)-2, the forward primer was 5′-GCGTTCTGGAGACCATGGA-3′ and reverse was 5′-ACAAAGTTGCTCTGAAAACAAATCA-3′, the amplicon size is 131 bp; for SREBP-1c, the forward primer was 5′-GGAGCCATGGATTGCACATT-3′ and reverse was 5′-GCTTCCAGAGAGGAGGCCAG-3′, the amplicon size is ~170 bp; for 3-hydroxy-3-methyl-glutaryl-CoA reductase (HMG-CoAR), the forward primer was 5′-CTTGTGGAATGCCTTGTGATTG-3′ and reverse was 5′-AGCCGAAGCAGCACATGAT-3′, the amplicon size is 76 bp; for fatty acid synthase (FAS), the forward primer was 5′-GCTGCGGAAACTTCAGGAAAT-3′ and reverse was 5′-AGAGACGTGTCACTCCTGGACTT-3′, the amplicon size is 84 bp; for β-actin, the forward primer was 5′-GGCACCACACCTTCTACAATG-3′ and the reverse was 5′-GGGGTGTTGAAGGTCTCAAAC-3′; the amplicon size is 132 bp. For GRP78, the forward primer was 5′-ACCTGGGTGGGGAAGACTTT-3′ and reverse was 5′-TCTTCAAATTTGGCCCGAGT-3′, the amplicon size is 232 bp; for PDI, the forward primer was 5′-AACGGGAGAAGCCATTGTA-3′

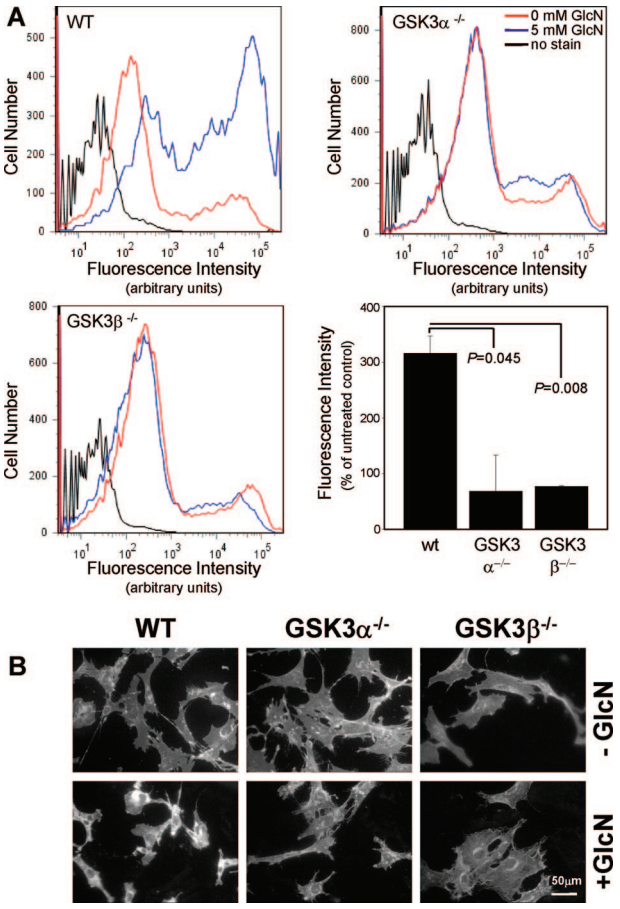

Figure 2. The effect of GSK-3 deficiency on glucosamine-induced lipid accumulation. Wild-type, GSK-3$\alpha^{-/-}$, and GSK-3$\beta^{-/-}$ MEFs were challenged with 0 or 5 mmol/L glucosamine for 18 hours. Cells were stained with filipin and fluorescence was examined by FACS (**A**) and fluorescence microscopy (**B**). For FACS, >10,000 cells were analyzed from each treatment group using excitation wavelengths of 350 to 370 nm and emission detection at 420 to 460 nm.

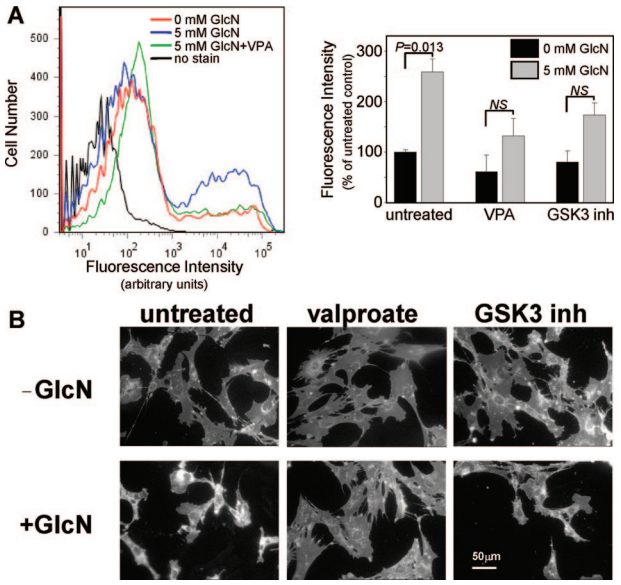

Figure 3. The effect of GSK-3 inhibition on glucosamine-induced lipid accumulation. Wild-type MEFs were challenged with 0 or 5 mmol/L glucosamine in the presence of valproate or 200 μmol/L GSK-3 inhibitor II. Cells were stained with filipin and analyzed by FACS (**A**) and fluorescence microscopy (**B**) as described in Figure 2.

and reverse was 5′-AGGTGTCATCCGTCAGCTCT-3′, the amplicon size is 156 bp; for spliced XBP-1, the forward primer was 5′-GTCCGCAGCAGGTGCAG-3′ and reverse was 5′-GGGAGTTCCTCCAGACTAGC-3′, the amplicon size is 177 bp; for CHOP, the forward primer was 5′-GTCCCTAGCTTGGCTGACAGA-3′ and the reverse was 5′-TGGAGAGCGAGGGCTTTG-3′. The standard method was used for the quantification of the mRNA expression in the livers using β-actin as a normalization control gene.

Immunohistochemical Analysis

Mice were euthanized, hearts were flushed with 1× PBS, and perfusion-fixed with 10% neutral buffered formalin. After removal, hearts, including the aortic root, were cut transversely and embedded in paraffin. Serial sections (4 μm) of aortic root were collected on precoated glass slides for measurement of lesion size (hematoxylin and eosin staining) or immunohistochemical staining.[32] The Vectastain ABC System (Vector Laboratories, Burlingame, CA) was used for immunohistochemical analysis. Sections were stained with primary antibodies and visualized using appropriate biotinylated secondary antibodies and Nova Red. Nonspecific staining was controlled for using a similar section and pre-immune IgG. Images were captured with a charge-coupled device color video camera (Sony, Tokyo, Japan) and analyzed using Northern Exposure (Empix, Tonawanda, NY) and SigmaScan Pro software.

Lipid Staining

Liver cryosections, 7 μm thick, were collected on slides and fixed in formal calcium for 30 minutes. Neutral lipids were visualized in sections that were rinsed and incubated in a saturated, filtered solution of Oil Red O (Sigma) for 7 minutes. After rinsing with H_2O, nuclei were stained with hematoxylin, and slides were mounted in Crystal-mount.[33] Relative amounts of lipid staining were quantified using Image J 1.35 Software (National Institutes of Health, Bethesda, MD).

Immunoblot Analysis of Mouse Liver Proteins

Cytoplasmic proteins were isolated from mouse liver using a NE-PER kit (Pierce, Rockford, IL) and total protein lysates were prepared from mouse liver solubilized in RIPA buffer. Equivalent amounts of total protein were separated on sodium dodecyl sulfate-polyacrylamide gels and transferred to nitrocellulose membranes (Bio-Rad, Hercules, CA), as described previously.[10,33] After incubation with the appropriate primary and horseradish peroxidase-conjugated secondary antibodies, the membranes were developed using the Immobilon Western chemiluminescent horseradish peroxidase substrate (Millipore). Specific bands were quantified using the Typhoon 9410 Imaging System (GE Healthcare, Waukesha, WI).

Table 1. Metabolic Parameters in ApoE$^{-/-}$ Mice

	Experimental group			
	Control	Control + valproate	HG	HG + valproate
Body weight (g)	20.9 ± 1.8	20.9 ± 1.1	19.5 ± 0.6	20.1 ± 1.6
Liver weight (g)	0.85 ± 0.1	0.80 ± 0.9	0.88 ± 0.13	0.94 ± 0.21
Lesion volume (10^{-3}mm^3)	3.80 ± 0.55	3.21 ± 0.56	8.62 ± 1.23*	4.98 ± 0.76†
Mac-3-positive cells/section	24.5 ± 6.9	26.8 ± 7.0	30.3 ± 7.2*	16.1 ± 5.2†
Plasma				
Valproate (μmol/L)	0	37.5 ± 14.9	0	33.7 ± 6.2
Fasting glucose (12 hours) (mmol/L)	4.3 ± 0.7	4.7 ± 0.5	7.6 ± 2.1‡	8.3 ± 2.7‡
Fed glucose (mmol/L)	14.0 ± 2.7	12.6 ± 3.5	23.2 ± 5.6‡	27.0 ± 0.9‡
Cholesterol (mmol/L)	11.6 ± 2.1	13.1 ± 3.7	12.7 ± 3.1	13.5 ± 3.5
Triglyceride (mmol/L)	0.21 ± 0.06	0.28 ± 0.10	0.41 ± 0.26*	0.29 ± 0.14

HG, hyperglycemic; n = 9 to 16 per treatment group for each measurement.
* $P < 0.05$ relative to control mice fed the nonsupplemented (control) diet.
† $P < 0.05$ relative to HG mice fed control diet.
‡ $P < 0.05$ relative to control mice fed the same diet.

GSK-3β Activity Assay

GSK-3β was immunoprecipitated from total protein lysates prepared from mouse liver. Kinase activity was measured by monitoring the incorporation of ^{32}P onto phospho-glycogen synthase peptide-2 (pGS-2; Upstate, Billerica, MA) as previously described.[34]

Statistical Analysis

Results are presented as the mean ± SD. One-way analysis of variance was used for repeated measurements of the same variable, and Duncan's multiple range *t*-test was used to assess differences between experimental groups and controls. Probability values of <0.05 were considered statistically significant.

Results

The UPR in Wild-Type and GSK-3-Deficient MEFs

Conditions of ER stress have previously been associated with increased GSK-3 activity in various rodent cells.[23–26] However the effect of GSK-3 deficiency on the ability of a cell to initiate the UPR is not known. To determine whether GSK-3 α/β activity is directly involved in the UPR, we challenged wild-type MEFs and MEFs that are deficient in GSK-3α or GSK-3β with ER stress-inducing agents, including tunicamycin (10 μg/ml), the calcium ionophore A23187 (7 μmol/L), and glucosamine (5 mmol/L) for 18 hours and measured the induction of specific UPR proteins (Figure 1 and see Supplemental Figure S1 at *http://ajp.amjpathol.org*). The results indicate that each of the MEF cell lines respond to various ER stress-inducing agents by significantly increasing the levels of GRP78 and GADD153. Basal levels of calreticulin are relatively high in the MEFs, and the fold induction under conditions of ER stress is not significant. These findings suggest that GSK-3α and GSK-3β do not play essential roles in the induction of the UPR in MEFs.

The Effect of GSK-3α and -3β Deficiency on ER Stress-Induced Cholesterol Accumulation

It has been established that conditions of ER stress can promote cholesterol accumulation in specific cell types including hepatocarcinoma cells.[10] We examined the potential role of GSK-3 activity in this response using the GSK-3-deficient MEFs. Filipin staining of MEFs treated with glucosamine was analyzed using FACS and fluorescence microscopy (Figure 2). Results show that exposure to 5 mmol/L glucosamine induces significant unesterified cholesterol accumulation in wild-type MEFs but not in GSK-3$\alpha^{-/-}$ or GSK-3$\beta^{-/-}$ MEFs. This effect appears to be ER stress-specific because the GSK-3-deficient MEFs do accumulate unesterified cholesterol when exposed to U18666A, a chemical that blocks intracellular trafficking of cholesterol, thereby activating cholesterol biosynthesis (see Supplemental Figure S2 at *http://ajp.amjpathol.org*).[35] These findings suggest that both the α and β GSK-3 isoforms play a specific role in ER stress-induced unesterified cholesterol accumulation.

Effect of GSK-3 Inhibitors on Glucosamine-Induced Lipid Accumulation in Wild-Type MEFs

We have previously shown that the branched chain fatty acid, valproate, can inhibit both recombinant and intracellular GSK-3α/β activity.[10,34] We have also shown that valproate and other GSK-3 inhibitors attenuate ER stress-associated unesterified cholesterol accumulation and apoptosis in cultured HASMCS and HepG2 cells (see Supplemental Figure S3 at *http://ajp.amjpathol.org*).[10] Here we examine the effect of valproate, and a potent maleimide-based GSK-3 inhibitor, on glucosamine-induced cholesterol accumulation in wild-type MEFs. FACS analysis of filipin-stained wild-type MEFs indicates that glucosamine-induced unesterified cholesterol accumulation is significantly lower in cells pretreated with valproate or GSK-3 inhibitor II (Figure 3). This result is consistent with the previous findings suggesting that GSK-3 activity plays a role in ER stress-associated unesterified cholesterol accumulation.

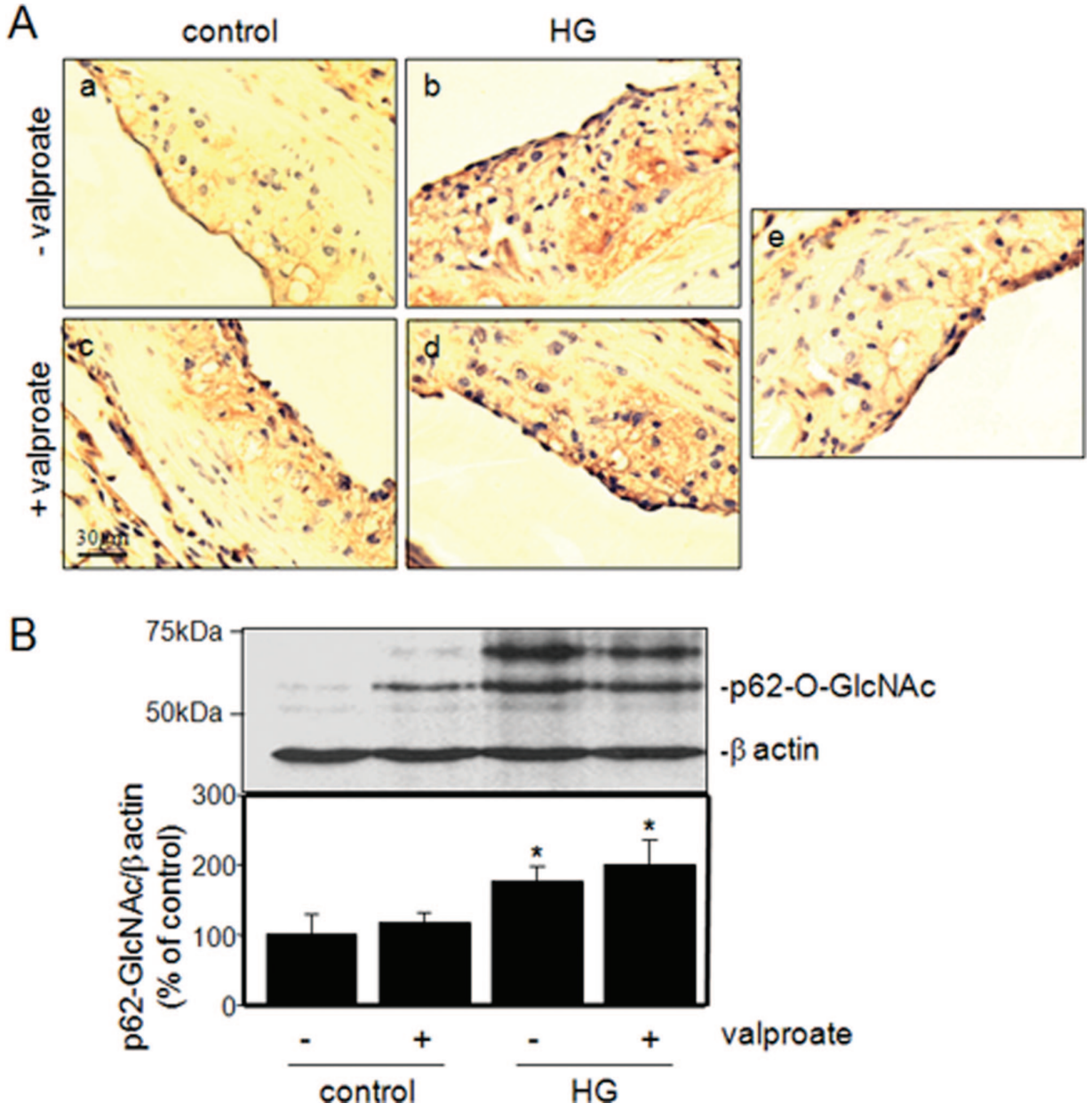

Figure 4. Effect of valproate supplementation on intracellular O-linked glycosylation. **A:** Representative sections of aortic root of control female normoglycemic and hyperglycemic apoE$^{-/-}$ mice fed control diet (**a**, **b**) or control diet supplemented with sodium valproate (**c**, **d**) were stained with an antibody against O-linked *N*-acetylglucosamine (CTD110.6) or pre-immune IgG (**e**). **B:** Total protein lysates from liver were analyzed by immunoblot analysis using the RL-2 antibody. The relative amounts of the O-glycosylated nuclear pore protein, p62 (p62-O-GlcNAc), an established marker of intracellular glucosamine levels, were quantified and plotted for each group. $n = 3$ to 6 per group; $^{*}P < 0.05$ relative to controls.

Induction of Hyperglycemia in ApoE$^{-/-}$ Mice

Hyperglycemia was induced in female apoE$^{-/-}$ mice by multiple low-dose intraperitoneal injections of STZ.[9,31] Blood glucose levels were monitored weekly in all experimental groups. All STZ-injected mice were hyperglycemic by the time of the last injection. At the time of sacrifice (15 weeks of age), 12-hour fasting plasma glucose concentration in STZ-injected mice was 7.6 ± 2.1 mmol/L versus 4.3 ± 0.7 mmol/L ($P < 0.05$) in control mice (Table 1).

Effect of Hyperglycemia and Dietary Valproate Supplementation on Metabolic Parameters

Supplementation of defined mouse chow with 625 mg/kg of sodium valproate increased plasma valproate levels to

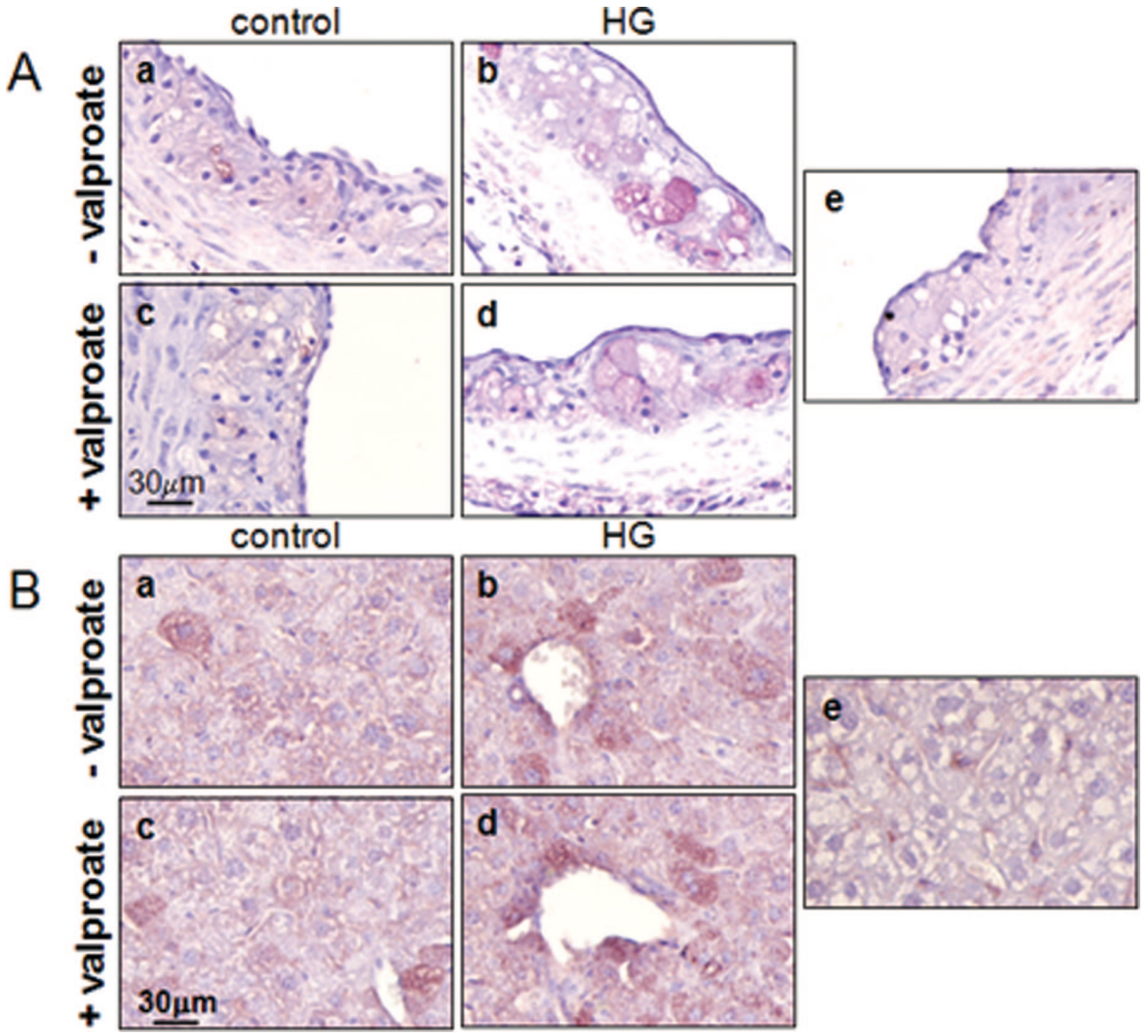

Figure 5. Effect of valproate on markers of ER stress. **A:** Representative sections of aortic root from each of the indicated treatment groups were immunostained with antibodies against phosphorylated-PERK (**a–d**) or pre-immune IgG (**e**). **B:** Sections of liver from each of the treatment groups were immunostained with anti-KDEL antibody (**a–d**) or pre-immune IgG (**e**) as indicated.

37.5 ± 14.9 μmol/L in control apoE$^{-/-}$ mice (Table 1). Plasma valproate levels were not significantly different in hyperglycemic apoE$^{-/-}$ mice relative to normoglycemic mice. Valproate supplementation had no significant effect on body or liver weight in any of the experimental groups relative to age-matched mice fed control diet. In addition there was no significant effect on fasting and fed plasma glucose [10 weeks (data not shown) or 15 weeks (Table 1)], plasma cholesterol (Table 1), or lipid profile (data not shown) as a result of valproate supplementation. Consistent with previous studies, the induction of hyperglycemia did not significantly affect plasma cholesterol levels in 15-week-old apoE$^{-/-}$ mice.[9] These findings indicate that this level of valproate supplementation is subsymptomatic, which is consistent with previous preclinical analysis of valproate toxicity in rodents.[36]

When dietary levels of sodium valproate were increased to 1250 mg/kg chow, corresponding plasma valproate levels increased to 131.4 ± 10.1 μmol/L. This level of supplementation did correspond to a significant decrease in plasma glucose levels in STZ-treated apoE$^{-/-}$ mice (from 23.2 ± 5.6 to 13.1 ± 2.0 mmol/L, $P < 0.05$). The diet containing the lower (625 mg/kg) concentration of sodium valproate was used in all subsequent experiments.

Effects of Hyperglycemia and Valproate on Hepatic Levels of O-Linked Protein Glycosylation

Glucosamine is a product of glucose flux through the hexosamine pathway and an ER stress-inducing agent that we have previously linked to diabetic atherogenesis.[9,10] Alterations in intracellular glucosamine concentration were determined by evaluating the extent of O-linked glycosylation, as described previously.[9,13] Hyperglycemic mice have elevated levels of O-linked *N*-acetyl glycosylation (GlcNAc) in aortae relative to control mice (Figure 4). The supplementation of diet with sodium valproate did not affect the observed levels of O-linked glycosylation in cells of the vascular lesions (Figure 4A). This result is supported by quantification of O-linked glycosylated protein p62 in liver

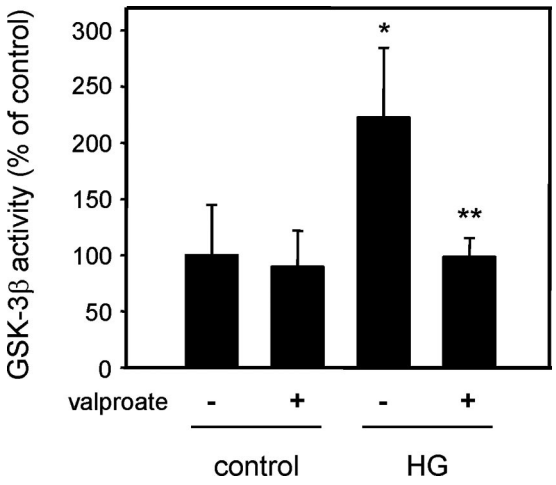

Figure 6. Effect of valproate supplementation on hepatic GSK-3 activity. GSK-3β was immunoprecipitated from protein lysates prepared from the livers of normoglycemic (control) and hyperglycemic (HG) mice fed control or valproate-supplemented diet. GSK-3β kinase activity was determined as previously described.[10] $n = 3$, $^{*}P < 0.05$ relative to nonsupplemented control. $^{**}P < 0.05$ relative to nonsupplemented HG.

by immunoblot analysis (Figure 4B).[13] These findings are consistent with the similar blood glucose concentrations observed in supplemented and nonsupplemented mice.

Effect of Hyperglycemia and Valproate on Diagnostic Markers of ER Stress

Liver and aortic cross sections from mice in each of the treatment groups were immunostained with an anti-KDEL antibody, directed against GRP78/94, or an anti-phospho-PERK antibody. Consistent with our previous findings, hyperglycemia correlates with increased protein levels of KDEL and phospho-PERK staining in smooth muscle cells and macrophages that make up the vascular lesion (Figure 5A). Dietary supplementation with sodium valproate did not significantly affect the protein levels of these ER stress markers in atherosclerotic lesions of control or hyperglycemic mice. Similar results were observed by immunohistochemical analysis in the livers from the same experimental groups (Figure 5B). The expression levels of hepatic ER stress response genes were also examined using real time RT-PCR (see Supplemental Figure S4 at *http://ajp.amjpathol.org*). Results indicate that mRNA transcripts encoding ER stress response genes are significantly elevated in hyperglycemic mice and that supplementation with sodium valproate attenuates this effect.

Effect of Valproate Supplementation on Hepatic GSK-3β Activity

GSK-3β was immunoprecipitated from hepatic protein lysates from normoglycemic and hyperglycemic mice and kinase activity was determined as previously described.[34] GSK-3β kinase activity was significantly elevated in the liver of hyperglycemic mice fed control diet compared to normoglycemic mice (Figure 6). Hepatic GSK-3β activity in hyperglycemic apoE$^{-/-}$ mice fed valproate-supplemented diet was similar to the levels found in normoglycemic mice and significantly lower than hyperglycemic mice fed the control diet. This indicates that valproate can inhibit GSK-3β *in vivo*.

Effects of Valproate Supplementation on Hepatic Steatosis

Cryosections of liver isolated from each of the treatment groups were stained with Oil Red O (Figure 7A). Consistent with our previous findings, conditions of hyperglycemia promote the accumulation of hepatic lipids in apoE$^{-/-}$ mice.[9] Significantly reduced levels of hepatic lipid were present in hyperglycemic mice that received dietary supplementation with valproate relative to nonsupplemented controls (Figure 7B). This finding is supported by an observed increase in hepatic mRNA transcripts encoding proteins involved in lipid biosynthesis, including SREBP-1c, FAS, and HMG-CoA reductase, in hyperglycemic mice fed control diet. Hyperglycemic mice fed the valproate-supplemented diet had significantly lower levels of these transcripts (Figure 7C).

Effects of Valproate Supplementation on Atherosclerosis in Hyperglycemic Mice

Hyperglycemia significantly increased mean atherosclerotic lesion volume at the aortic root of apoE$^{-/-}$ mice relative to control apoE$^{-/-}$ mice (2.3-fold) (Figure 8 and Table 1), consistent with reported data.[37] Dietary supplementation with sodium valproate correlated to a significant decrease in cross-sectional lesion area and total mean lesion volume in hyperglycemic mice (4.98 ± 0.76 versus $8.62 \pm 1.23 \times 10^{-3}\text{mm}^3$, $P < 0.05$) relative to nonsupplemented controls (Figure 8 and Table 1). Hyperglycemic apoE$^{-/-}$ mice fed a diet supplemented with lithium (4 g $LiCO_3$/kg chow), a selective GSK-3 inhibitor, also had reduced lesion size at the cross section of aortic root compared to control diet-fed mice (see Supplemental Figure S5 at *http://ajp.amjpathol.org*). In hyperglycemic mice the reduced lesion volume corresponded with a significant reduction in the number of Mac-3-positive macrophages/foam cells within the atherosclerotic plaque (Table 1). A nonsignificant trend toward smaller lesion volume was observed in normoglycemic apoE$^{-/-}$ mice fed the valproate diet. In all mice, atherosclerotic lesion development was confined to a region within 120 μm of the aortic root and no lesions were observed in the descending aorta or the aortic arch of any of the treatment groups (data not shown).

Discussion

Independent cardiovascular risk factors, including hyperhomocysteinemia, hyperglycemia, cholesterol accumula-

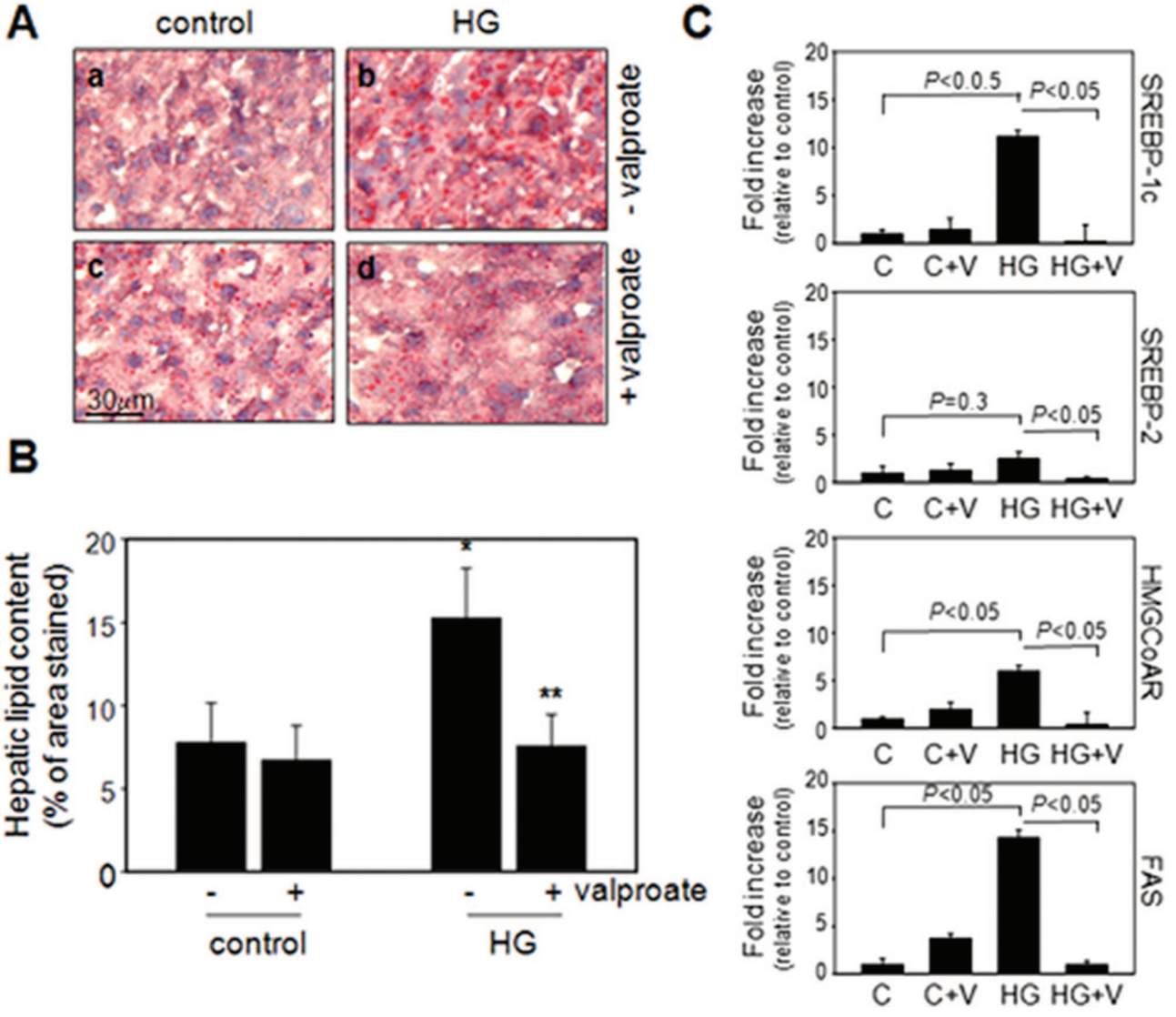

Figure 7. Effect of valproate supplementation on hepatic steatosis. **A:** Representative sections of liver from control or hyperglycemic apoE$^{-/-}$ mice fed control diet or valproate-supplemented diet, as indicated, were stained with Oil Red O. **B:** Quantification of Oil Red O staining in representative cross sections. $n = 3$ per group. **C:** Quantification of mRNA levels using quantitative RT-PCR in the liver lysates from indicated groups. $^{*}P < 0.05$ relative to control mice, $^{**}P < 0.05$ relative to mice from the same treatment group without valproate supplementation.

tion, and obesity, have been associated with increased levels of ER stress in hepatocytes, adipocytes, and cells of the artery wall in several different murine models.[6–9,33] Recent data suggest that there is a direct correlation between vascular ER stress levels and the accelerated development of atherosclerotic lesions in hyperhomocysteinemic and hyperglycemic apoE$^{-/-}$ mice.[6,9]

In this study we begin to identify the molecular links by which ER stress may promote atherosclerosis and present evidence that GSK-3 plays a central role in the transmission of pro-atherogenic signals under conditions of hyperglycemia. *In vitro*, we show that MEFs deficient in GSK-3 have a similar UPR but are resistant to ER stress-induced cholesterol accumulation relative to wild-type MEFs, supporting a role of GSK-3 subsequent to ER stress but preceding cellular dysfunctions. *In vivo* we show that STZ-induced hyperglycemic apoE$^{-/-}$ mice have increased GSK-3 activity, elevated ER stress levels, hepatic steatosis, and significantly enlarged atherosclerotic lesion volume relative to normoglycemic controls. Dietary supplementation with valpoate, a molecule with GSK-3 inhibitory properties,[17,34] normalizes hepatic GSK-3 activity, reduces hepatic steatosis, and attenuates accelerated atherosclerosis in this model. Together these findings suggest that conditions of hyperglycemia may activate ER stress response pathways that signal through GSK-3 to dysregulate cholesterol metabolism and perhaps activate other pro-atherosclerotic pathways.

The present study is based on previous results showing that elevated concentrations of glucose and glu-

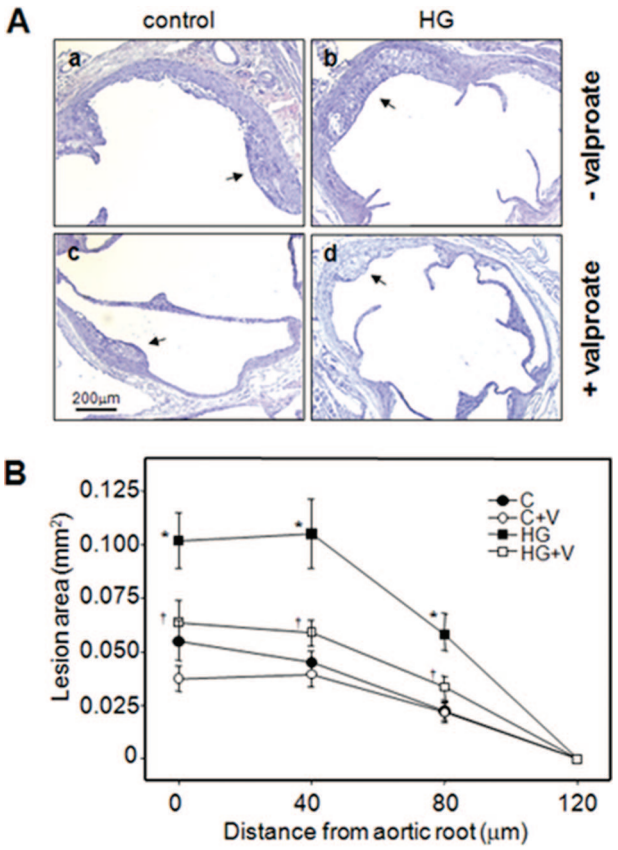

Figure 8. Effect of valproate supplementation on atherosclerotic plaque area in hyperglycemic apoE-deficient mice. **A:** Representative H&E-stained aortic root cross sections from 15-week-old control female normoglycemic and hyperglycemic apoE$^{-/-}$ mice fed control diet (**a**, **b**) or control diet supplemented with sodium valproate (**c**, **d**) as indicated. **B:** Lesion areas were determined at the aortic root (0 μm) and at 40-μm intervals in aortae isolated from control (C) or hyperglycemic (HG) mice fed control diet or control diet supplemented with sodium valproate (+V). $n = 9$ to 10 per group; $^{*}P < 0.05$, relative to control mice; $^{\dagger}P < 0.05$, relative to similar treatment group in the absence of valproate supplementation. **Arrows** indicate atherosclerotic lesions.

cosamine can promote ER stress in cultured hepatocytes, vascular smooth muscle cells, and macrophages.[9] We and others have demonstrated that ER stress can lead to caspase activation and programmed cell death in cultured endothelial cells,[38,39] and SREBP activation and subsequent lipid accumulation in HASMCs and hepatocytes.[33,40] Exposure of cultured HASMCs, Thp-1, and HepG2 cells to glucosamine promotes a robust ER stress response and the induction of nuclear factor-κB and SREBP activity.[9,10] The molecular mechanisms by which glucosamine disrupts ER homeostasis and the pathways by which ER stress activate pro-atherogenic responses are not fully understood.

It has been previously reported that ER stress-inducing agents, including thapsigargin and brefeldin A, increase GSK-3 activity in human neuroblastoma cells,[22] mouse insulinoma cells,[23] MEFs,[24] and rat cerebral cortical cells.[25,26] The mechanism by which GSK-3 is activated possibly involves the dephosphorylation of phospho-Ser-9 of GSK-3β, an event that switches GSK-3 from an inactive to an active kinase.[22,23,25] ER stress-induced GSK-3 activity promotes caspase-dependent apoptosis in neuronal cells, and pretreatment with lithium or small molecule inhibitors of GSK-3 is sufficient to protect cells from ER stress-induced programmed cell death.[22,25,26]

Valproate is a widely prescribed drug in the treatment of epilepsy and bipolar disorder; however, the mechanism(s) by which valproate alleviates convulsions and modifies behavior remain controversial.[18,41] Valproate has many intracellular effects that may be responsible for its clinical efficacy. These include its ability to potentiate GABA-mediated postsynaptic inhibition,[42] to promote the depletion of intracellular inositol,[43] to inhibit histone deacetylase (HDAC) activity,[44] to promote the expression of protein chaperones,[10,45] and to directly and/or indirectly inhibit GSK-3 activity.[17,19,34] We have shown that exposure to valproate can protect cultured cells, including HepG2 and HASMCs, from ER stress-induced lipid accumulation and apoptosis.[10] The ability of valproate-derived compounds to attenuate ER stress-induced lipid accumulation correlates directly with their ability to inhibit GSK-3 (see Supplemental Figure S3 at *http://ajp.amjpathol.org*). The ability of other established GSK-3 inhibitors, such as alsterpaullone and a synthetic bisaryl-maleimide,[26] to attenuate ER stress-induced cellular dysfunction supports a role for GSK-3 in ER stress signaling.

Increased GSK-3β activity has been reported in skeletal muscle from humans with type 2 diabetes[27] and adipose tissue from C57BL/6 mice with diet-induced diabetes.[28] We have determined that hepatic GSK-3β activity in STZ-induced hyperglycemic apoE$^{-/-}$ mice is more than twofold higher than normoglycemic controls. This increase corresponds to an elevation of intracellular glucosamine levels [1.8-fold ($P < 0.05$) increase in O-linked GlcNAc] and a similar increase in hepatic ER stress levels as well as a twofold ($P < 0.05$) elevation in hepatic lipid content. Hepatic steatosis is characteristic of hyperglycemic rodent models[9,46] and is also a complication associated with diabetes mellitus in humans.[47] We propose that glucosamine-induced ER stress promotes hepatic lipid accumulation by a pathway that involves GSK-3 activation. This model is supported by the findings that GSK-3$^{-/-}$ MEFs do not accumulate unesterified cholesterol under conditions of ER stress (Figure 2) and that hyperglycemic mice fed a valproate-supplemented diet have a significant reduction in hepatic GSK-3β activity (Figure 6) and hepatic lipid levels (Figure 7), but no change in ER stress levels (Figure 5) relative to nonsupplemented hyperglycemic mice.

It is well established that STZ-induced hyperglycemia promotes accelerated atherosclerosis in apoE$^{-/-}$ mice.[9,31] As with hepatic steatosis, accelerated atherosclerosis is associated with increased levels of glucosamine and ER stress in the cells of the vascular lesion (Figures 4 and 5).[9] Here we show that dietary supplementation with valproate is associated with significantly reduced lesion volume in hyperglycemic mice but not in normoglycemic mice.

It is not clear at this time if the vascular and hepatic effects of valproate supplementation are mechanistically linked or are independent phenomena. Hepatic GSK-3β activity is clearly reduced in supplemented mice relative to controls (Figure 6); however, it was not possible to

determine vascular activity because of the limited amount of tissue available. Therefore, it is possible that valproate indirectly inhibits atherogenesis by altering hepatic lipid metabolism, although the fact that plasma lipid levels are not significantly affected suggests that the effects of valproate are a result of localized action. It is important to note that the plasma valproate concentration attained in this mouse model is ~10 times lower than clinically relevant plasma concentrations for the treatment of epilepsy in humans (0.28 to 0.7 mmol/L[48]). There is no clear correlation between valproate use and cardiovascular disease or incidence of myocardial infarction in human populations, although any association is likely complicated by weight gain that is observed in humans but not in rodents taking valproate.[48,49]

Together these findings suggest that the observed hepatic, and perhaps vascular, effects of dietary supplementation result from the ability of valproate to attenuate the increase in GSK-3 activity observed under conditions of hyperglycemia. We hypothesize that conditions of hyperglycemia accelerate atherogenesis by a pathway involving ER stress-induced GSK-3 activity and that valproate attenuates this effect by directly or indirectly inhibiting GSK-3 signaling.

Although the data presented here is consistent with this hypothesis, there are several other potential explanations for the observed effect. First, it has been shown that GSK-3 inhibition by lithium can have some insulin mimetic effects involving stimulation of glucose uptake and glycogen synthesis in adipose and muscle cells.[50,51] However, we observed no significant changes in plasma glucose levels or intracellular O-linked glycosylation in mice supplemented with 625 mg/kg of valproate suggesting that this mechanism is not playing a major role. Second, the recognized ability of valproate to affect other intracellular enzymes and pathways could produce effects that slow or block atherogenesis. Valproate is a known HDAC inhibitor and it is therefore possible that valproate confers athero-protection by altering gene expression patterns through the inhibition of HDAC.[44,52] The HDAC inhibitor, trichostatin (TSA), has been shown to inhibit vascular smooth muscle cell proliferation[53] but actually exacerbates atherosclerosis in an LDL receptor-deficient mouse model.[54] We observed no significant difference in hepatic histone acetylation in any of the mouse treatment groups suggesting that HDAC activity was unaffected by hyperglycemia and the concentration of plasma valproate induced by supplementation (data not shown). Exposure to valproate is known to increase the expression of cellular chaperones including HSP70, GRP78, HSP47, protein disulfide isomerase (PDI), and calreticulin in rat neurons and in cultured HepG2 cells.[10,45] Overexpression of GRP78 or calreticulin can protect certain cells from stress-induced dysfunction.[33,55] Furthermore, a recent report has shown that small molecule chaperones can alleviate ER stress and improve glucose homeostasis and insulin sensitivity in a mouse model of type 2 diabetes.[7] However, no significant increase in ER chaperone expression was observed in liver or aortae of mice fed the valproate diet, and we have shown *in vitro*[10] and *in vivo* that exposure to valproate does not significantly affect the protein levels of diagnostic markers of ER stress in cells and tissue (Figure 5). We conclude that valproate must confer its cytoprotective properties by acting subsequent to the induction of ER stress and the UPR. Finally, it must be noted that valproate can be metabolized into a complex array of intermediates,[56] any one of which may be acting as the direct effector on one or more of these pathways. Further studies will be required to more clearly determine which, if any, of these factors and mechanisms are directly responsible for the observed athero-protective effect.

Identification of the factors and pathways that mechanistically link diabetes mellitus to cardiovascular disease is vital to our understanding of the molecular mechanisms of disease development and progression. The validation of a pro-atherogenic role for ER stress and the specific involvement of GSK-3 will facilitate the identification of other potential targets and small molecule interventions toward the goal of developing effective therapies to treat and prevent cardiovascular disease.

Acknowledgments

We thank Dr. Bradley Doble for providing MEF cell lines and Vimarsha Swami for assistance with the manuscript.

References

1. Haffner SM, Lehto S, Ronnemaa T, Pyorala K, Laakso M: Mortality from coronary heart disease in subjects with type2 diabetes and in nondiabetic subjects with and without prior myocardial infarction. N Engl J Med 1998, 339:229–234
2. Nathan DM, Lachin J, Cleary P, Orchard T, Brillon DJ, Backlund JY, O'Leary DH, Genuth S; and the Diabetes Control and Complications Trial; Epidemiology of Diabetes. N Engl J Med 2003, 348:2294–2303
3. Turner RC, Holman RR, Cull CA, Stratton IM, Matthews DR, Frighi V, Manley SE, Neil A, McElroy H, Wright D, Kohner E, Fox C, Hadden D, and the UK Prospective Diabetes. Lancet 1998, 352:837–853
4. Standl E, Balletshofer B, Dahl B, Weichenhain B, Steigler H, Hormann A, Holl R: Predictors of 10-year macrovascular and overall mortality in patients with NIDDM: the Munich General Practitioner Project. Diabetologia 1996, 39:1540–1545
5. Marciniak SJ, Ron D: Endoplasmic reticulum stress signaling in disease. Physiol Rev 2006, 86:1133–1149
6. Zhou J, Werstuck GH, deKoning ABL, Hossain GS, Sood SK, Shi YY, Moller J, Ritskes-Hoitinga M, Falk E, Austin RC: Association of multiple cellular stress pathways with accelerated atherosclerosis in hyperhomocysteinemic ApoE-deficient mice. Circulation 2004, 110:207–213
7. Özcan U, Cao Q, Yilmaz E, Lee A-H, Iwakoshi NN, Özdelen E, Tuncman G, Görgun C, Glimcher LH, Hotamisligil GS: Endoplasmic reticulum stress links obesity, insulin action, and type 2 diabetes. Science 2004, 306:457–461
8. Li Y, Schwabe RF, Devries-Seimon T, Yao PM, Gerbod-Giannone MC, Tall AR, Davis RJ, Flavell R, Brenner DA, Tabas I: Free cholesterol-loaded macrophages are an abundant source of TNF-alpha and IL-6. Model of NF-kappa B- and MAP kinase-dependent inflammation in advanced atherosclerosis. J Biol Chem 2005, 280:21763–21772
9. Werstuck GH, Khan MI, Femia G, Kim AJ, Tedesco V, Trigatti B, Shi YY: Glucosamine-induced endoplasmic reticulum stress is associated with accelerated atherosclerosis in a hyperglycemic mouse model. Diabetes 2005, 55:93–101
10. Kim AJ, Shi YY, Austin RC, Werstuck GH: Valproate protects cells from endoplasmic reticulum stress-induced lipid accumulation and apoptosis by inhibiting glycogen synthase kinase 3. J Cell Sci 2005, 118:89–99
11. Kockeritz L, Doble B, Patel S, Woodgett JR: Glycogen synthase

kinase-3—an overview of an over-achieving protein kinase. Curr Drug Targets 2006, 7:1377–1388
12. Jope RS, Yuskaitis CJ, Beurel E: Glycogen synthase kinase-3 (GSK3): inflammation, diseases, and therapeutics. Neurochem Res 2007, 32:577–595
13. Han I, Oh E, Kudlow JE: Responsiveness of the state of O-linked N-acetylglucosamine modification of nuclear pore protein p62 to the extracellular glucose concentration. Biochem J 2000, 350:109–114
14. Meares GP, Jope RS: Resolution of the nuclear localization mechanism of glycogen synthase kinase-3: functional effects in apoptosis. J Biol Chem 2007, 282:16989–17001
15. Hoeflich KP, Luo J, Rubie EA, Tsao MS, Jin O, Woodgett JR: Requirement for glycogen synthase kinase-3beta in cell survival and NF-kappaB activation. Nature 2000, 406:86–90
16. Gong R, Rifai A, Ge Y, Chen S, Dworkin LD: Hepatocyte growth factor suppresses proinflammatory NF{kappa}B activation through GSK3{beta} inactivation in renal tubular epithelial cells. J Biol Chem 2008, 283:7401–7410
17. Chen G, Huang L-D, Jiang Y-M, Manji HK: The mood-stabilizing agent valproate inhibits the activity of glycogen synthase kinase-3. J Neurochem 1999, 72:1327–1330
18. Bowden CL, Brugger AM, Swann AC, Calabrese JR, Janicak PG, Petty F, Dilsaver SC, Davis JM, Rush AJ, Small JG, Garza-Trevino ES, Risch SC, Goodnick PJ, Morris DD: Efficacy of divalproex vs lithium and placebo in the treatment of mania. The Depakote Mania Study Group. JAMA 1994, 271:918–924
19. De Sarno P, Li X, Jope RS: Regulation of Akt and glycogen synthase kinase-3 beta phosphorylation by sodium valproate and lithium. Neuropharmacology 2002, 43:1158–1164
20. Liu Z, Tanabe K, Bernal-Mizrachi E, Permutt MA: Mice with beta cell overexpression of glycogen synthase kinase-3beta have reduced beta cell mass and proliferation. Diabetologia 2008, 51:623–631
21. Tanabe K, Liu Z, Patel S, Doble BW, Li L, Cras-Méneur C, Martinez SC, Welling CM, White MF, Bernal-Mizrachi E, Woodgett JR, Permutt MA: Genetic deficiency of glycogen synthase kinase-3beta corrects diabetes in mouse models of insulin resistance. PLoS Biol 2008, 6:307–318
22. Song L, De Sarno P, Jope RS: Central role of glycogen synthase kinase-3β in endoplasmic reticulum stress-induced caspase-3 activation. J Biol Chem 2002, 277:44701–44708
23. Srinivasan S, Ohsugi M, Liu Z, Fatrai S, Bernal-Mirachi E, Permutt MA: Endoplasmic reticulum stress-induced apoptosis is partly mediated by reduced insulin signaling through phosphatidylinositol 3-kinase/Akt and increased glycogen synthase kinase-3beta in mouse insulinoma cells. Diabetes 2005, 54:968–975
24. Pluquet O, Qu LK, Baltzis D, Koromilas AE: Endoplasmic reticulum stress accelerates p53 degradation by the cooperative actions of Hdm2 and glycogen synthase kinase 3beta. Mol Cell Biol 2005, 25:9392–9405
25. Brewster JL, Linseman DA, Bouchard RJ, Loucks FA, Precht TA, Esch EA, Heidenreich KA: Endoplasmic reticulum stress and trophic factor withdrawal activate distinct signaling cascades that induce glycogen synthase kinase-3 beta and a caspase-9-dependent apoptosis in cerebellar granule neurons. Mol Cell Neurosci 2006, 32:242–253
26. Takadera T, Fujibayahi M, Kaniyu H, Sakota N, Ohyashiki T: Caspase-dependent apoptosis induced by thapsigargin was prevented by glycogen synthase kinase-3 inhibitors in cultured rat cortical neurons. Neurochem Res 2007, 32:1336–1342
27. Nikoulina SE, Ciaraldi TP, Mudaliar S, Mohideen P, Carter L, Henry RR: Potential role of glycogen synthase kinase-3 in skeletal muscle insulin resistance of type 2 diabetes. Diabetes 2000, 49:263–271
28. Eldar-Finkelman H, Schreyer SA, Shinohara MM, LeBoeuf RC, Krebs EG: Increased glycogen synthase kinase-3 activity in diabetes- and obesity-prone C57BL/6J mice. Diabetes 1999, 48:1–5
29. Ciaraldi TP, Oh DK, Christiansen L, Nikoulina SE, Kong AP, Baxi S, Mudaliar S, Henry RR: Tissue-specific expression and regulation of GSK-3 in human skeletal muscle and adipose tissue. Am J Physiol 2006, 291:E891–E898
30. Kruth HS: Histochemical detection of esterified cholesterol within human atherosclerotic lesions using the fluorescent probe filipin. Atherosclerosis 1984, 51:281–292
31. Kunjathoor VV, Wilson D, LeBoeuf RC: Increased atherosclerosis in streptozotocin-induced diabetic mice. J Clin Invest 1996, 97: 1767–1773
32. Paigen B, Morrow A, Holmes PA, Mitchell D, Williams RA: Quantitative assessment of atherosclerotic lesions in mice. Atherosclerosis 1987, 68:231–240
33. Werstuck GH, Lentz SR, Dayal S, Shi Y, Hossain GS, Sood SK, Krisans SK, Austin RC: Homocysteine causes dysregulation of the cholesterol and fatty acid biosynthesis pathways. J Clin Invest 2001, 107:1263–1273
34. Werstuck GH, Kim AJ, Brenstrum T, Ohnmacht SA, Panna E, Capretta A: Examining the correlations between GSK-3 inhibitory properties and anticonvulsant efficacy of valproate and valproate-derived compounds. Bioorg Med Chem Lett 2004, 14:5465–5467
35. Underwood KW, Andemariam B, McWilliams GL, Liscum L: Quantitative analysis of hydrophobic amine inhibition of intracellular cholesterol transport. J Lipid Res 1996, 37:1556–1568
36. Walker RM, Smith GS, Barsoum NJ, Macallum GE: Preclinical toxicology of the anticonvulsant calcium valproate. Toxicology 1990, 63:137–155
37. Levi Z, Shaish A, Yacov N, Levkovitz H, Trestman S, Gerber Y, Cohen H, Dvir A, Rhachmani R, Ravid M, Harats D: Rosiglitazone (PPARγ-agonist) attenuates atherogenesis with no effect on hyperglycaemia in a combined diabetes-atherosclerosis mouse model. Diabetes Obes Metab 2003, 5:45–50
38. Hossain GS, van Thienen JV, Werstuck GH, Zhou J, Sood SK, Dickhout JG, de Koning AB, Tang D, Wu D, Falk E, Poddar R, Jacobsen DW, Zhang K, Kaufman RJ, Austin RC: TDAG51 is induced by homocysteine, promotes detachment-mediated programmed cell death and contributes to the development of atherosclerosis in hyperhomocysteinemia. J Biol Chem 2003, 278:30317–30327
39. Kim KM, Pae HO, Zheng M, Park R, Kim YM, Chung HT: Carbon monoxide induces heme oxygenase-1 via activation of protein kinase R-like endoplasmic reticulum kinase and inhibits endothelial cell apoptosis triggered by endoplasmic reticulum stress. Circ Res 2007, 101:919–927
40. Lee JN, Ye J: Proteolytic activation of SREBP induced by cellular stress through the depletion of Insig-1. J Biol Chem 2004, 279:45257–45265
41. Penry JK, Dean JC: The scope and use of valproate in epilepsy. J Clin Psychiatry 1989, 50:17–22
42. MacDonald RL, Bergey GK: Valproic acid augments GABA-mediated postsynaptic inhibition in cultured mammalian neurons. Brain Res 1979, 170:558–562
43. Williams RSB, Cheng L, Mudge AW, Harwood AJ: A common mechanism of action for three mood-stabilizing drugs. Nature 2002, 417:292–295
44. Phiel CJ, Zhang F, Huang EY, Guenther MG, Lazar MA, Klein PS: Histone deacetylase is a direct target of valproic acid, a potent anticonvulsant, mood stabilizer, and teratogen. J Biol Chem 2001, 276:36734–36741
45. Wang J-F, Bown C, Young LT: Differential display PCR reveals novel targets for the mood-stabilizing drug valproate including the molecular chaperone GRP78. Mol Pharmacol 1999, 55:521–527
46. Ohno T, Horio F, Tanaka S, Terada M, Namikawa T, Kitoh J: Fatty liver and hyperlipidemia in IDDM (insulin-dependent diabetes mellitus) of streptozotocin-treated shrews. Life Sci 2000, 66:125–131
47. Clark JM, Brancati FL, Diehl AM: Nonalcoholic fatty liver disease. Gastroenterology 2002, 122:1649–1657
48. Guerrini R: Valproate as a mainstay of therapy for pediatric epilepsy. Paediatr Drugs 2006, 8:113–129
49. Wolden-Hanson T, Gidal BE, Atkinson RL: Evaluation of a rat model of valproate-induced obesity. Pharmacotherapy 1998, 18:1075–1781
50. Tabata I, Schluter J, Gulve EA, Holloszy JO: Lithium increases susceptibility of muscle glucose transport to stimulation by various agents. Diabetes 1994, 43:903–907
51. Oreña SJ, Torchia AJ, Garofalo RS: Inhibition of glycogen-synthase kinase 3 stimulates glycogen synthase and glucose transport by distinct mechanisms in 3T3–L1 adipocytes. J Biol Chem 2000, 275:15765–15772
52. Göttlicher M, Minucci S, Zhu P, Kramer OH, Schimpf A, Giavara S, Sleeman JP, Lo Coco F, Nervi C, Pelicci PG, Heinzel T: Valproic acid defines a novel class of HDAC inhibitors inducing differentiation of transformed cells. EMBO J 2001, 20:6969–6978
53. Okamoto H, Fujioka Y, Takahashi A, Takahashi T, Taniguchi T, Ishikawa Y, Yokoyama M: Trichostatin A, an inhibitor of histone deacetylase, inhibits smooth muscle cell proliferation via induction of p21(WAF1). J Atheroscler Thromb 2006, 13:183–191

54. Choi JH, Nam KH, Kim J, Baek MW, Park JE, Park HY, Kwon HJ, Kwon OS, Kim DY, Oh GT: Trichostatin A exacerbates atherosclerosis in low density lipoprotein receptor-deficient mice. Arterioscler Thromb Vasc Biol 2005, 25:2404–2409
55. Liu H, Miller E, van de Water B, Stevens JL: Endoplasmic reticulum stress proteins block oxidant-induced Ca2+ increases and cell death. J Biol Chem 1998, 273:12858–12862
56. Tong V, Teng XW, Chang TKH, Abbott FS: Valproic acid 1: time course of lipid peroxidation biomarkers, liver toxicity, and valproic acid metabolite levels in rats. Toxicol Sci 2005, 86:427–435